

ARTICLE



## Multiparametric ultrasonographic analysis of testicular tumors: a single-center experience in a collective of 49 patients

Vincent Schwarze<sup>a</sup>, Constantin Marschner<sup>a</sup>, Bastian Sabel<sup>a</sup>, Giovanna Negrão de Figueiredo<sup>a</sup>, Julian Marcon<sup>b</sup>, Michael Ingrisch<sup>a</sup>, Thomas Knösel<sup>c</sup>, Johannes Rübenthaler<sup>a</sup> and Dirk-André Clevert<sup>a</sup>

<sup>a</sup>Department of Radiology, Ludwig-Maximilians-University Munich – Grosshadern Campus, Munich, Germany; <sup>b</sup>Department of Urology, Ludwig-Maximilians-University Munich – Grosshadern Campus, Munich, Germany; <sup>c</sup>Institute of Pathology, Ludwig-Maximilians-University Munich – Grosshadern Campus, Munich, Germany

### ABSTRACT

**Purpose:** The aim of the present retrospective single-center study is to evaluate the diagnostic performance of multiparametric ultrasonography for characterizing testicular tumors.

**Method:** Forty-nine patients with testicular tumors, 36 of malignant vs 13 of benign entity, were included in this retrospective single-center study on whom multiparametric sonography, encompassing native B-mode, Color Doppler, contrast-enhanced ultrasound (CEUS) and elastography, was performed between 2011–2018. In 48 of 49 patients, findings from multiparametric analysis were correlated with histopathological results. The applied contrast agent for CEUS was a second-generation blood pool agent. Ultrasonography examinations were performed and interpreted by a single experienced radiologist with more than 15 years of experience (EFSUMB Level 3).

**Results:** Multiparametric ultrasonography was successfully performed in all included patients without any adverse effects. Concomitant testicular microlithiasis, rapid arterial wash-in, elevated values for perfusion quantification – Peak Enhancement (PE), Wash-in Area Under the Curve (WiAUC) and Wash-in Perfusion Index (WiPI) – and higher shear wave velocities were significantly associated with malignancy.

**Conclusions:** Multiparametric ultrasonography depicts a non-ionizing, directly accessible and cost-effective imaging modality that allows for the extensive characterization of testicular tumors, thereby helping to discriminate between malignant and benign entity of testicular tumors.

### ARTICLE HISTORY

Received 14 March 2020

Revised 19 April 2020

Accepted 4 May 2020

### KEYWORDS

Testicular tumor; seminoma; contrast-enhanced ultrasound; elastography; multiparametric ultrasound

## Introduction

Malignant testicular tumors comprise up to 1% of all malignant tumors in men and constitute the most common solid tumor entity in young adult men [1]. The incidence of testicular cancer has increased during the past two decades [2]. Developed countries have higher rates than developing countries. Ninety percent of testicular tumors are germ cell tumors [3,4], which are subclassified as seminomatous and non-seminomatous tumors, the former being the most frequent of all histological subtypes. Primary and secondary non-germ cell tumors are distinguished, e.g. Leydig cell tumor or metastases, respectively.

Amongst benign differentials which may mimic testicular cancer are cysts, hemangioma, adenomatoid tumors or inflammatory conditions [5,6].

Cryptorchidism, a positive family history and testicular cancer in the contralateral testis depict known risk factors for the development of testicular malignancy [7,8].

An accurate non-invasive analysis of the testicular lesion is critical for facilitating adequate therapy and for preventing unnecessary surgical intervention.

Due to its cost-effectiveness, direct accessibility, high spatial and temporal resolution and its excellent safety profile, ultrasonography is the imaging modality of choice for the dynamic assessment of testicular symptoms and pathologies. The combined use of native B-mode and Color Doppler proved high diagnostic accuracy in detecting testicular lesions [5], but is limited when it comes to further delineating the underlying entity. Several studies could show that, by further evaluating the tumor stiffness by real-time elastography (RTE) malignant tumors are often associated with increased stiffness compared to the surrounding testicular parenchyma due to their enhanced cell density. What is more, upon intravenous application of microbubbles, contrast-enhanced-ultrasound (CEUS) enables us to visualize intratumoral microperfusion in testicular tumors and thus further characterizes benign and malignant lesions [9].

The European Association of Urology (EAU) recommends timely diagnostic ultrasonography to evaluate possible underlying scrotal pathology [10]. The European Federation of Societies for Ultrasound in Medicine and Biology (EFSUMB) recommends the use of contrast-enhanced ultrasound (CEUS)

for differentiating vascularized from non-vascularized focal testicular lesions [11]. Nevertheless, there are still no established valid sonomorphologic features which allow for safe differentiation between malignant or benign origin.

As a more elaborate imaging modality, MRI of the testes allows for precise determination of the tumor category (T) of the TNM staging system and depicts the second level imaging modality for scrotal analysis [12]. The staging of testicular cancer is further arranged by combining histopathological results, levels of serum tumor markers which include alpha-fetoprotein (AFP) and human chorionic gonadotrophin (hCG), CT of the chest and CT or MRI of the abdomen. In the case of conspicuous neurological signs imaging of the brain should be conducted [13]. Most patients with testicular malignancy are being diagnosed in stages of localized disease. The 5-year overall survival rate is 95.3%.

The aim of the present single-center study was to assess the diagnostic performance of multiparametric analysis of testicular tumors.

## Materials and methods

This retrospective single-center study was approved by the local institutional ethical committee of the institutional review board and all contributing authors followed the ethical guidelines for publication in *Scandinavian Journal of Urology*. All study data were gathered according to the principles expressed in the Declaration of Helsinki/Edinburgh 2002. Oral and written informed consent of all patients were given before CEUS examination and their associated risks and potential complications have been carefully described. All CEUS examinations were performed and analyzed by a single skilled radiologist with more than 15 years of clinical experience (EFSUMB Level 3). All included patients underwent native B-mode, Color Doppler, CEUS scans and strain elastography (SE) or shear wave elastography (SWE). Up-to-date high-end ultrasound systems with adequate CEUS protocols were utilized (GE Healthcare: LOGIQ E9; Samsung RS80A Prestige, Siemens Ultrasound Sequoia S20000, S3000, Philips Ultrasound iU22, EPIQ 7). A low mechanical index was used to avoid early destruction of microbubbles ( $<0.2$ ). For all CEUS examinations, the second-generation blood pool contrast agent *SonoVue*<sup>®</sup> (Bracco, Milan, Italy) was used. 1.0–2.4 ml of *SonoVue*<sup>®</sup> were applied. After contrast agent was applied, a bolus of 5–10 ml sterile 0.9% sodium chloride solution was given. No adverse side-effects upon administration of *SonoVue*<sup>®</sup> were registered. All CEUS examinations were successfully performed and image quality was sufficient in every single case allowing for proper analysis of the sonomorphological appearance of the testicular lesions. The patient files and imaging records were retrieved from the picture archiving and communication system (PACS) of our institution.

Evaluation of morphological features of the testicular tumors in native B mode included: location, size, shape and echogenicity of the tumors and testicular microlithiasis. Vascularization was evaluated using Color Doppler and CEUS. Additional elastographic evaluation, either by shear wave

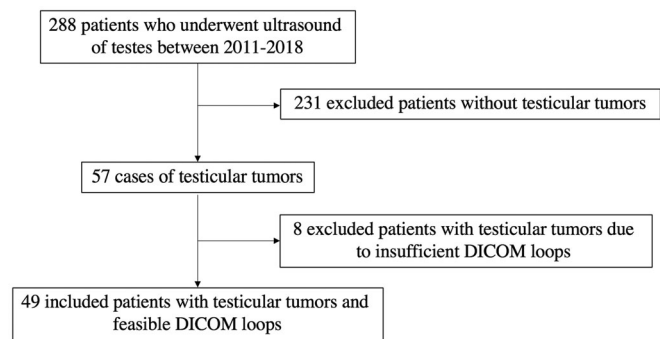


Figure 1. Flowchart illustrating included and excluded patients.

elastography (SWE) or strain elastography (SE), was performed in each case. For assessing tissue stiffness by SE, repeated compression and decompression of the testis by the probe was performed. In strain elastography stiffness of malignant and benign lesions and surrounding testicular parenchyma were visualized by color coding in real-time. Stiffness was classified as 'hard', 'soft' or 'equivalent' compared to surrounding parenchyma. In SWE, a 3 mm diameter region-of-interest (ROI) was placed in the longitudinal plane in native B-mode into the testicular lesions and surrounding parenchyma. At least three shear wave velocity (SWV) measurements were performed in each examined case.

Between 2011–2018, 288 men underwent ultrasonographic examination of the testes, of whom 49 patients with testicular tumors were included in the study (Figure 1). DICOM loops from eight patients with testicular tumors were not feasible for appropriate analysis due to moving artifacts or limited duration. All included patients with unknown testicular lesions were retrieved by full text search in our archiving clinical database and PACS system. All patients agreed on participation in clinical trials during medical care at our University Hospital. Multiparametric analysis – encompassing native B-mode, Color Doppler, CEUS and elastography – was performed in every patient (Table S1).

Forty-eight of 49 patients underwent (partial) orchiectomy in the local Department of Urology. The histopathological analysis was performed in collaboration with the local Institute of Pathology. Histopathological results were used as the diagnostic gold standard.

Perfusion quantification was performed using the quantification software *VueBox*<sup>®</sup> (Bracco Suisse SA - Software Applications, Geneva, Switzerland) by using DICOM cine loops. After initial software calibration (depending on ultrasound transducers, presets, gain) regions of interest (ROI) were manually placed: first, the delimitation ROI, ROI1 into the testicular parenchyma as reference and ROI2 into the testicular tumor were set. ROIs did not change during the entire clip. Quantitative perfusion analysis was performed and parameters of interest were Peak-Enhancement (PE), Rise Time (RT), Time to Peak (TTP), Wash-in Area Under the Curve (WiAUC), Wash-in Rate (WIR), Wash-in Perfusion Index (WiPI), mean Transit Time local (mTTI), Wash-out AUC (WoAUC), Wash-in and Wash-out-AUC (WiWoAUC), Fall Time (FT), Wash-out Rate (WoR) and Quality of Fit (QOF).

Statistical analysis was performed by using *Graph Pad Prism* (GraphPad Software Inc., La Jolla, CA). For qualitative comparison of morphologic features seen in native B-mode, Color Doppler mode and CEUS in malignant vs benign lesions chi-squared ( $\chi^2$ ) test was performed. Wilcoxon's matched *t*-test was used for comparing quantified perfusion data of malignant and benign lesions with corresponding surrounding testicular parenchyma. Quantified perfusion data of malignant and benign lesions were normalized to surrounding non-neoplastic testicular parenchyma and quantified using Mann-Whitney test. Statistical analysis of shear wave velocity (SWV) values in malignant and benign lesions compared to corresponding normal testicular parenchyma was performed using Wilcoxon's matched *t*-test. Mann-Whitney test was used for comparison of SWV values in malignant vs benign lesions. Statistical tests were considered significant if *p*-value < 0.05.

## Results

Multiparametric ultrasonographic examination was performed in all patients without the occurrence of any adverse effects. The mean age of the patients at the time of CEUS performance was 46 years (min = 7; max = 80). In one patient bilateral lesions as manifestations of diffuse large b-cell lymphoma were found. In 34 patients, lesions were located in the left testicle (27 malignant vs 7 benign lesions, 79% vs 21%) and, in 14 patients, lesions were located in the right testicle (8 malignant vs 6 benign lesions, 57% vs 43%). The mean size of testicular tumors was 1.2 cm (min = 0.2; max = 8.0 cm). The mean size of benign and malignant tumors was 0.9 cm (min = 0.3; max = 3.0 cm) and 1.4 cm (min = 0.3 cm; max = 8.0 cm), respectively. There was no significant difference in mean diameters of malignant vs benign tumors and in age between patients with malignant lesions and in patients with benign lesions. The underlying histopathological subtypes of the included malignant (*n* = 36) and benign (*n* = 13) testicular lesions are illustrated in Table 1, with seminoma and Leydig cell tumors being the most frequent malignant and benign tumors, respectively.

The sonomorphological features of the included malignant and benign lesions were analyzed and compared using native B-mode, Color Doppler and CEUS (Table 2). In our collective, characterizing the echogenicity of testicular lesions by native B-mode showed a high specificity of 1.0 (0/13 benign lesions were hyperechoic, 13/13 benign lesions were hypoechoic). Inhomogeneous echogenicity, well-demarcated or blurred margins of testicular tumors were not significantly associated with either malignant or benign entity.

A higher prevalence of microlithiasis was detected in malignant tumors than in benign tumors, in 21/36 malignant tumors vs in 3/13 benign tumors (*p* = 0.0293) with a specificity of 0.77. When comparing the internal and peripheral vascularization of the intratesticular lesions by Color Doppler, no significant difference between malignant and benign tumors was observed, but malignant tumors tended to feature hypervascularization more frequently than benign tumors (Table 2).

**Table 1.** Clinical characteristics of included patients related to subtype of testicular tumor (Malignant tumors and benign tumors).

Subtype	Numbers	Mean age	Mean diameter	R	L	B
<i>Malignant tumors</i>						
Seminoma	21 (58)	40	1.4	6	15	0
Mixed	4 (11)	25	1.0	0	4	0
Embryonal carcinoma	3 (8)	35	2.4	1	2	0
Hematologic manifestation	3 (8)	50	0.9	0	2	1
Teratoma	2 (6)	19	1.0	1	1	0
Metastasis	2 (6)	68	1.9	0	2	0
Yolk sac tumor	1 (3)	33	0.6	0	1	0
<i>Benign tumors</i>						
Leydig cell tumor	7 (54)	41	0.6	1	6	0
Sertoli cell tumor	2 (15)	39	0.4	1	1	0
Cyst	1 (8)	25	0.2	1	0	0
Adenomatoid tumor	1 (8)	51	1.2	1	0	0
Fibroid pseudotumor	1 (%)	56	1.5	1	0	0
Epidermoid cyst	1 (8)	37	3.0	1	0	0

R, right; L, left; B, both. Numbers of tumors depicted as absolute numbers and percentages in parentheses. Mean age in years. Mean diameter in cm.

**Table 2.** Comparison of sonomorphologic features of malignant and benign testicular tumors of the study cohort. Malignant tumors (*n* = 36), benign tumors (*n* = 13) in absolute numbers and percentages in parentheses.

	Malignant	Benign	$\chi^2$	<i>p</i> -value	Sens.	Spec.
<i>B-mode US</i>						
<i>Echogenicity</i>						
Hyperechoic	7 (19)	0	3.149	0.076	0.194	1.00
Hypoechoic	29 (81)	13 (100)			0.81	1.00
Inhomogeneous	17 (47)	3 (23)	2.305	ns	0.47	0.77
<i>Margins</i>						
Well-demarcated	8 (22)	4 (31)	0.3773	ns	0.22	0.69
Blurred	28 (78)	9 (69)			0.78	0.31
<i>Microlithiasis</i>						
Parenchymal	3 (8.3)	0	1.154	ns	0.08	1.0
Intralesional	5 (14)	2 (15)	0.01745	ns	0.01	0.69
Both	13 (36)	1 (8)	3.258	ns	0.36	0.92
None	15 (42)	10 (77)	4.751	0.0293	0.42	0.23
Cumulative	21 (58)	3 (23)	4.751	0.0293	0.58	0.77
<i>Doppler</i>						
<i>Vascularization</i>						
Internal	10 (28)	3 (23)	0.1083	ns	0.28	0.77
Peripheral	3 (8.3)	0	1.154	ns	0.08	1.0
Both	17 (47)	5 (38)	0.2963	ns	0.47	0.38
Cumulative	30 (83)	8 (62)	2.606	ns	0.83	0.62
<i>CEUS</i>						
Rapid Wash-in	33 (92)	9 (69)	3.926	0.0475	0.92	0.31
Delayed Wash-in	1 (3)	1 (8)	0.5892	ns	0.03	0.08
None	1 (3)	3 (23)	5.25	0.0220	0.03	0.77
Wash-out	2 (6)	0	0.753	ns	0.06	1.00

US: ultrasound; Sens: sensitivity; Spec: specificity; CEUS: contrast-enhanced ultrasound. ns: not significant.

Despite the heterogeneity of the two patient cohorts, the registration of rapid wash-in in testicular lesions was significantly associated with malignant entities (in 33/36 malignant lesions vs 9/13 benign lesions, *p* = 0.0475). Reciprocally, absence of wash-in was more often seen in benign lesions (1/36 malignant lesions vs 3/13 lesions, *p* = 0.0220). Wash-out was detected in 2/36 malignant tumors and in none of the benign tumors (Figure 2(D)).

Perfusion quantification parameters of malignant and benign tumors are shown in Table 3. Significantly higher values for PE, WiPI and WiR were observed in malignant compared to benign tumors (*p* = 0.0466, *p* = 0.0260, *p* = 0.0421, respectively). In juxtaposition with the surrounding

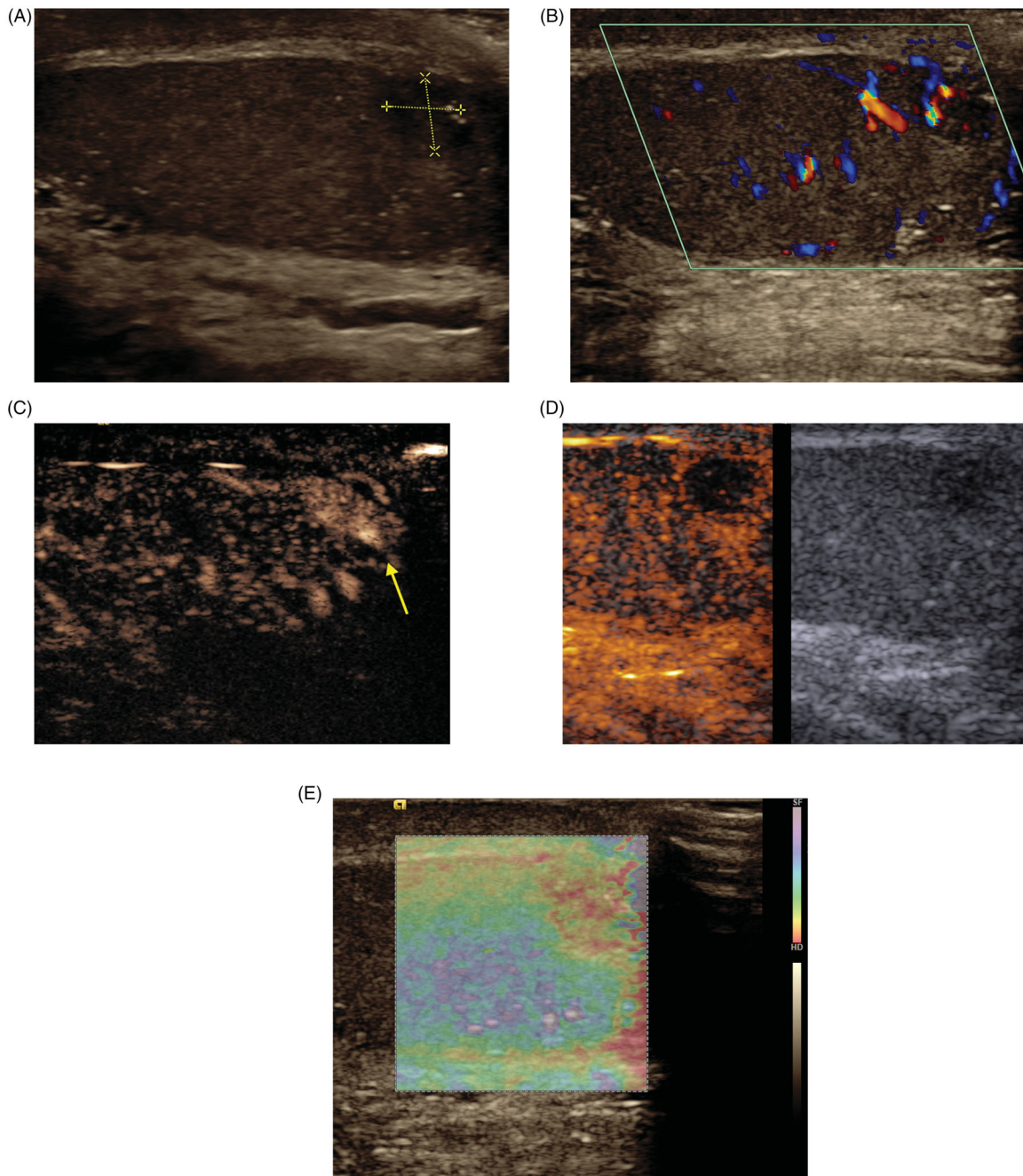


**Figure 2.** Sonomorphologic appearance of testicular embryonal carcinoma. Native B-mode shows an unclear 0.5 cm hypoechoic lesion in the inferior pole of the left testicle (A). Intralesional and peripheral hypervascularization is depicted in Color Doppler mode (B). Rapid early contrast enhancement of the lesion is registered in CEUS (C, yellow arrow). Subsequently, delayed wash-out of the lesion is registered in CEUS (D, left, corresponding native B-mode shown right). Elevated stiffness of the tumor is revealed by strain elastography (E).

unaffected testicular parenchyma, malignant and benign tumors featured significantly higher levels for PE, WiAUC, WiPI, TTP, WiR, WoAUC, WiWoAUC and WoR.

Except for one patient (pat. #14) in whom equivalent stiffness between Sertoli cell tumor and surrounding testicular parenchyma was registered, all included benign and malignant lesions presented hard in SE (malignant lesions:  $n = 20$ , benign lesions:  $n = 8$ ).

Shear wave elastography revealed significantly increased shear wave velocity (SWV) values in malignant lesions ( $n = 15$ , mean SWV = 2.98 m/s, range = 1.38–5.68 m/s) compared to corresponding adjacent normal testicular

parenchyma (mean SWV = 1.15 m/s, range = 0.59–1.91 m/s) ( $p < 0.0001$ ). No significant difference between SWV values of benign lesions ( $n = 5$ , mean SWV = 1.7 m/s, range = 1.40–2.20 m/s) compared to surrounding normal testicular parenchyma (mean SWV = 0.89 m/s, range = 0.7–1.6 m/s) was registered ( $p = 0.0625$ ). Moreover, malignant testicular lesions (mean SWV = 3.08 m/s, range = 2.17–5.68 m/s) presented significantly higher SWV values than benign lesions (mean SWV = 1.7 m/s, range = 1.19–2.2 m/s) ( $p < 0.0001$ ) (Figure 3A). Seminomas (mean SWV = 2.74 m/s, range = 2.06–4.28 m/s) featured significantly elevated SWV values in comparison with surrounding normal testicular tissue (mean

**Table 3.** Perfusion quantification parameters of malignant and benign testicular tumors.

Parameter	Malignant tumors	Benign tumors	Malignant vs benign tumor – <i>p</i> -value*	Malignant tumor vs parenchyma – <i>p</i> -value	Benign tumor vs parenchyma – <i>p</i> -value
PE	3,505.3 (20–42,500)	234.0 (176–7,020)	0.0466	<0.0001	0.0002
WiAUC	13,403.9 (31.3–105,000)	4,470.3 (398–14,700)	ns	<0.0001	0.0005
WiPI	1,916.1 (1.2–26,600)	1,178.5 (36.7–3,790)	0.0260	<0.0001	0.0002
RT	6.4 (0.2–18.4)	6.8 (1.7–10.8)	ns	ns	ns
mTTI	66.9 (0.7–527)	40.8 (3.7–90.4)	ns	ns	ns
TTP	9.9 (0.3–21.6)	11.7 (1.8–28.1)	ns	0.0295	0.0215
WiR	1,178.9 (1.1–14,600)	629.7 (7.2–3,660)	0.0421	<0.0001	0.0002
WoAUC	700.3 (0.4–7,210)	9,780.3 (57.4–55,300)	ns	0.0031	0.0181
WiWoAUC	50,719.2 (94–411,000)	32,610.4 (995–123,000)	ns	<0.0001	0.0078
FT	12.3 (1.7–43.5)	17.3 (4.2–30.8)	ns	ns	ns
WoR	700.3 (0.4–7210)	152.3 (1.9–576)	ns	0.0002	0.0312
QOF	71.6 (0.4–99.1)	64.1 (0.3–99.0)	ns	0.0168	ns

\*Normalized to adjacent non-neoplastic parenchyma.

PE: Peak-Enhancement; RT: Rise Time; TTP: Time to Peak; WiAUC: Wash-in Area Under the Curve; WiR: Wash-in Rate; WiPI: Wash-in Perfusion Index; mTTI: mean Transit Time local; WoAUC: Wash-out AUC; WiWoAUC: Wash-in and Wash-out-AUC; FT: Fall Time; WoR: Wash-out Rate; QOF: Quality of Fit; ns: not significant.

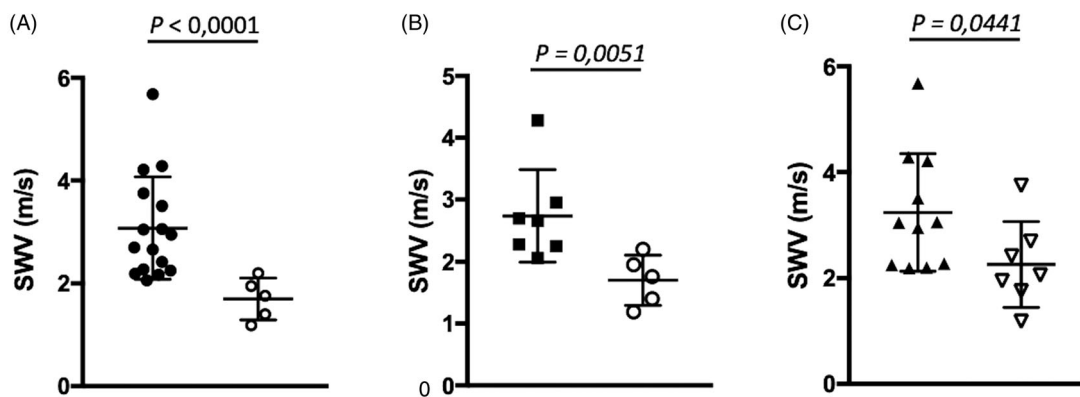


**Figure 3.** Analysis of shear wave elastography data illustrated as column graphs. Malignant lesions ( $n = 15$ , filled circles) feature significantly higher shear wave velocity (SWV) values compared to benign lesions ( $n = 5$ , unfilled circles),  $p < 0.0001$ , (A). Significantly elevated SWV values in seminomatous ( $n = 7$ , filled squares) vs non-seminomatous ( $n = 5$ , unfilled circles) lesions,  $p = 0.0051$  (B). Significantly increased SWV values of testicular lesions with concomitant testicular microlithiasis ( $n = 15$ , filled triangles) than in testicular lesions without microlithiasis ( $n = 7$ , unfilled triangles),  $p = 0.0441$  (C).

SWV = 1.11 m/s, range = 0.88–1.67 m/s) ( $n = 7$ ,  $p = 0.0156$ ). Juxtaposing seminomatous lesions ( $n = 7$ , mean SWV = 2.74 m/s, range = 2.06–4.28 m/s) to benign lesions (mean SWV = 1.7 m/s, range = 1.19–2.2 m/s) ( $n = 5$ ), significantly higher SWV values were observed in seminomas ( $p = 0.0051$ ) (Figure 3B). Testicular tumors with concomitant microlithiasis ( $n = 15$ , mean SWV = 3.24 m/s, range = 2.19–5.68 m/s) featured significantly higher SWV values than tumors without microlithiasis ( $n = 7$ , mean SWV = 2.26 m/s, range = 1.19–3.75 m/s) ( $p = 0.0441$ ) (Figure 3C).

The sonomorphologic appearance of a testicular embryonal carcinoma is illustrated in Figure 2.

## Discussion

In the past, the clinical examination of the testes had been the diagnostic method of choice for investigating scrotal pathologies. It depends strongly on the experience of the physician and frequently does not reveal the underlying pathology; particularly, very small lesions often are not palpable. At present, ultrasound is the primary imaging modality when it comes to evaluating the scrotum [4], thereby confining the limitations by mere clinical examination. The scrotum and testes are directly accessible and thus are especially feasible for ultrasonography. The testes may be affected by a

plethora of different pathologies, like infarctions, infections, hematologic manifestations, traumas or tumors.

Despite native B-mode and Color Doppler sonography depict high diagnostic accuracy in the detection of testicular masses, their capability in predicting histopathology frequently is limited [14]. Lesional hypervascularization registered in Color Doppler sonography may be associated with malignancy; however, as illustrated in Table 2, hypervascularization in Color Doppler is not a reliable sonomorphologic feature discriminating between malignant and benign tumors since benign lesions like Leydig cell tumors or Sertoli cell tumors often are hypervascularized.

The introduction and application of CEUS meant a significant refinement of the diagnostic performance of ultrasonography in the differential diagnosis of testicular pathologies [15]. Using CEUS, intratumoral microperfusion can dynamically be visualized at high spatial and temporal resolutions. It has previously been shown that neoplastic testicular lesions characteristically feature arterial hyperenhancement [9,16]. Absence of intratumoral vascularization is more likely associated with benign lesions [17]. Our findings go in line with the recent literature. In only three patients with malignant testicular lesions, no arterial enhancement could be registered by CEUS (Table 2). The histopathological correlation which revealed fibrotic seminoma (pat. #2), necrotic embryonal carcinoma (pat. #5) and necrotic teratoma (pat. #8)

clarified the lack of contrast enhancement in those tumors. Two testicular tumors featured malignancy-associated wash-out (Figure 2D), histopathological correlation revealed underlying seminoma and mixed germ-cell tumor (Table S1).

Commonly, intratesticular calcifications are detected during the sonographic examination of the scrotum [18], but the etiopathogenesis still remains unclear. Several clinical studies described that often spots of microlithiasis (<3 mm) are registered in germ-cell tumors [19,20].

Nevertheless, there is no valid information till now that microlithiasis depicts a premalignant condition [21]. Within the scope of the present study, we could observe a higher prevalence of microlithiasis in malignant tumors than in benign tumors, namely in 21/36 malignant tumors versus in 3/23 benign tumors ( $p=0.0293$ ) with a specificity of 0.77. However this finding might be explained due to the heterogeneity of the included tumor entities.

Strain elastography is the most frequent used technique to assess stiffness of the testes and testicular lesions to date. The ability of SE to distinguish between tumorous and non-tumorous lesions – like orchitis, partial infarctions or cysts – was already described [22]. Moreover, several studies analyzed and compared the elastographic findings of benign and malignant lesions [6,23–25]. In line with findings from the literature, compared to the surrounding testicular parenchyma the majority of testicular lesions in our study population appeared stiff in SE, only one Sertoli-cell lesion featured equivalent to surrounding normal testicular tissue elasticity. Findings from elastography alone frequently fail to determine the underlying entity of testicular lesions, e.g. cysts or hematoma may feature hard areas, thus be mistaken for malignant tumors (Table 1). Accordingly, additional sonographic features need to be investigated to assess the underlying entity.

Shear wave elastography is another technique to assess stiffness of testicular lesions [26–30]. Our findings go in line with a recent study which demonstrated significantly elevated stiffness in patients with testicular malignancy compared to normal surrounding parenchyma [31]. What is more, our results show significantly increased stiffness in malignant and benign testicular lesions compared to adjacent normal testicular parenchyma. Furthermore, as reported previously, SWE may allow for differentiating between malignant and benign lesions and between seminomas and non-seminomatous tumors [31,32].

Likewise, our findings demonstrate significantly higher stiffness of malignant lesions than of benign lesions (Figure 3A). In addition, the SWE evaluation of the included patients in our cohort revealed significantly higher stiffness in seminomatous lesions compared to surrounding parenchyma ( $p=0.0156$ ), and non-seminomatous lesions ( $p=0.0051$ ). Our findings indicate that SWE is a critical adjunct tool in the multiparametric scrutiny of the testes.

Comparable to the previously reported elevated stiffness in testicular lesions with concomitant microlithiasis in a pediatric collective, the analysis of SWE data in our patient collective revealed significantly elevated stiffness of testicular lesions with microlithiasis ( $p=0.0441$ ).

Along with the recent state of knowledge, our results show that a sophisticated multiparametric scrutiny of testicular lesions by ultrasonographic imaging techniques is crucial and may allow for close follow-up examinations or parenchyma-sparing surgery instead of radical orchiectomy [33]. Of note, multiparametric sonography is an easily accessible and non-ionizing imaging modality which can be repeatedly applied. The excellent safety profile of multiparametric ultrasonography, including CEUS, makes it a feasible diagnostic tool which can safely be applied, even in children [34]. The lower financial costs and morbidity of ultrasonography in comparison with more elaborate imaging techniques like MRI imaging of the testes is of relevance. Before computed tomography (CT) or MR imaging may be performed, thorough protocols must be evaluated in advance – respecting comorbidities of the patients like thyroid gland imbalances or renal impairment – to guarantee adequate scans. Nonetheless, ultrasonography cannot replace more elaborate imaging modalities in terms of tumor staging.

Limitations of the present study are the retrospective study design by which patients were in- and excluded. The heterogeneity of the included subtypes of malignant and benign testicular tumors and small numbers for certain subtypes may limit the validity and differentiation of multiparametric ultrasound analysis between both groups. The heterogeneity of testicular tumors may be influenced by the fact that all patients had consulted the Department of Urology of one single University Hospital. However, our findings are in line with results from previous clinical studies. Multiparametric ultrasound was performed between 2011–2018 with various but up-to-date ultrasound systems being used at the time of examination. To guarantee appropriate comparison of perfusion quantification results standardized VueBox<sup>®</sup> software – using calibrating files for the corresponding ultrasound transducer/ultrasound devices – was used. Moreover, all multiparametric ultrasound examinations were performed by one single radiologist (EFSUMB level 3).

In conclusion, the findings of our retrospective single-center study demonstrate that, in addition to the medical history, the clinical examination of the patient and serum levels of tumor markers, multiparametric ultrasonography depicts an indispensable tool in the diagnostic workup of testicular tumors and plays an essential role for subsequent therapeutic management.

## Disclosure statement

The authors report no conflicts of interest.

## References

- [1] Cheng L, Albers P, Berney DM, et al. Testicular cancer. *Nat Rev Dis Primers*. 2018;4(1):29.
- [2] Trabert B, Chen J, Devesa SS, et al. International patterns and trends in testicular cancer incidence, overall and by histologic subtype, 1973–2007. *Andrology*. 2015;3(1):4–12.

- [3] Smith ZL, Werntz RP, Eggener SE. Testicular cancer: epidemiology, diagnosis, and management. *Med Clin North Am.* 2018;102(2): 251–264.
- [4] Schwarze V, Marschner C, Rubenthaler J, et al. Overview of ultrasound applications for assessing scrotal disorders. *J Ultrasound Med.* 2019;39(6):1041–1243.
- [5] Dogra VS, Gottlieb RH, Oka M, et al. Sonography of the scrotum. *Radiology.* 2003;227(1):18–36.
- [6] Bernardo S, Konstantatou E, Huang DY, et al. Multiparametric sonographic imaging of a capillary hemangioma of the testis: appearances on gray-scale, color Doppler, contrast-enhanced ultrasound and strain elastography. *J Ultrasound.* 2016;19(1): 35–39.
- [7] Moller H, Cortes D, Engholm G, et al. Risk of testicular cancer with cryptorchidism and with testicular biopsy: cohort study. *BMJ.* 1998;317(7160):729.
- [8] Moller H, Prener A, Skakkebaek NE. Testicular cancer, cryptorchidism, inguinal hernia, testicular atrophy, and genital malformations: case-control studies in Denmark. *Cancer Causes Control.* 1996;7(2):264–274.
- [9] Lock G, Schmidt C, Helmich F, et al. Early experience with contrast-enhanced ultrasound in the diagnosis of testicular masses: a feasibility study. *Urology.* 2011;77(5):1049–1053.
- [10] Albers P, Albrecht W, Algaba F, et al. [EAU guidelines on testicular cancer: 2011 update. European Association of Urology]. *Actas Urol Esp.* 2012;36(3):127–145.
- [11] Sidhu PS, Cantisani V, Dietrich CF, et al. The EFSUMB guidelines and recommendations for the Clinical Practice of Contrast-Enhanced Ultrasound (CEUS) in non-hepatic applications: update 2017 (long version). *Ultraschall Med.* 2018;39(2):e2–e44.
- [12] Parenti GC, Feletti F, Carnevale A, et al. Imaging of the scrotum: beyond sonography. *Insights Imaging.* 2018;9(2):137–148.
- [13] Albers P, Albrecht W, Algaba F, et al. EAU guidelines on testicular cancer: 2011 update. *Eur Urol.* 2011;60(2):304–319.
- [14] Horstman WG, Melson GL, Middleton WD, et al. Testicular tumors: findings with color Doppler US. *Radiology.* 1992;185(3):733–737.
- [15] Huang DY, Sidhu PS. Focal testicular lesions: colour Doppler ultrasound, contrast-enhanced ultrasound and tissue elastography as adjuvants to the diagnosis. *Br J Radiol.* 2012;85(1):S41–S53.
- [16] Lerchbaumer MH, Auer TA, Marticorena GS, et al. Diagnostic performance of contrast-enhanced ultrasound (CEUS) in testicular pathologies: single-center results. *Clin Hemorheol Microcirc.* 2019; 73(2):347–357.
- [17] Hedayati V, Sellars ME, Sharma DM, et al. Contrast-enhanced ultrasound in testicular trauma: role in directing exploration, debridement and organ salvage. *Br J Radiol.* 2012;85(1011): e65–e68.
- [18] Renshaw AA. Testicular calcifications: incidence, histology and proposed pathological criteria for testicular microlithiasis. *J Urol.* 1998;160(5):1625–1628.
- [19] Kragel PJ, Delvecchio D, Orlando R, et al. Ultrasonographic findings of testicular microlithiasis associated with intratubular germ cell neoplasia. *Urology.* 1991;37(1):66–68.
- [20] Derogee M, Bevers RF, Prins HJ, et al. Testicular microlithiasis, a premalignant condition: prevalence, histopathologic findings, and relation to testicular tumor. *Urology.* 2001;57(6):1133–1137.
- [21] Pedersen MR, Rafaelsen SR, Moller H, et al. Testicular microlithiasis and testicular cancer: review of the literature. *Int Urol Nephrol.* 2016;48(7):1079–1086.
- [22] Aigner F, De Zordo T, Pallwein-Prettner L, et al. Real-time sonoelastography for the evaluation of testicular lesions. *Radiology.* 2012;263(2):584–589.
- [23] Schroder C, Lock G, Schmidt C, et al. Real-time elastography and contrast-enhanced ultrasonography in the evaluation of testicular masses: a comparative prospective study. *Ultrasound Med Biol.* 2016;42(8):1807–1815.
- [24] Kachramanoglou C, Rafailidis V, Philippidou M, et al. Multiparametric sonography of hematologic malignancies of the testis: grayscale, color doppler, and contrast-enhanced ultrasound and strain elastographic appearances with histologic correlation. *J Ultrasound Med.* 2017;36(2):409–420.
- [25] Lock G, Schroder C, Schmidt C, et al. Contrast-enhanced ultrasound and real-time elastography for the diagnosis of benign Leydig cell tumors of the testis - a single center report on 13 cases. *Ultraschall in Med.* 2014;35(06):534–539.
- [26] Marcon J, Trottmann M, Rubenthaler J, et al. Three-dimensional vs. two-dimensional shear-wave elastography of the testes - preliminary study on a healthy collective. *Clin Hemorheol Microcirc.* 2016;64(3):447–456.
- [27] Marcon J, Trottmann M, Rubenthaler J, et al. Shear wave elastography of the testes in a healthy study collective - differences in standard values between ARFI and VTIQ techniques. *Clin Hemorheol Microcirc.* 2017;64(4):721–728.
- [28] Trottmann M, Marcon J, D'Anastasi M, et al. Shear-wave elastography of the testis in the healthy man – determination of standard values. *Clin Hemorheol Microcirc.* 2016;62(3):273–281.
- [29] Trottmann M, Marcon J, D'Anastasi M, et al. The role of VTIQ as a new tissue strain analytics measurement technique in testicular lesions. *Clin Hemorheol Microcirc.* 2014;58(1):195–209.
- [30] Yusuf G, Konstantatou E, Sellars ME, et al. Multiparametric sonography of testicular hematomas: features on grayscale, color Doppler, and contrast-enhanced sonography and strain elastography. *J Ultrasound Med.* 2015;34(7):1319–1328.
- [31] Pedersen MR, Moller H, Osther PJS, et al. Comparison of tissue stiffness using shear wave elastography in men with normal testicular tissue, testicular microlithiasis and testicular cancer. *Ultrasound Int Open.* 2017;3(4):E150–E155.
- [32] Dikici AS, Er ME, Alis D, et al. Is there any difference between seminomas and nonseminomatous germ cell tumors on shear wave elastography? A preliminary study. *J Ultrasound Med.* 2016; 35(12):2575–2580.
- [33] Passman C, Urban D, Klemm K, et al. Testicular lesions other than germ cell tumours: feasibility of testis-sparing surgery. *BJU Int.* 2009;103(4):488–491.
- [34] Piscaglia F, Bolondi L. The safety of Sonovue in abdominal applications: retrospective analysis of 23188 investigations. *Ultrasound Med Biol.* 2006;32(9):1369–1375.